

Aggregation of Crystallins Induced by Pulsed Laser UV Light (308 nm)

L. V. Soustov^a, E. V. Chelnokov^a, N. V. Sapogova^a, N. M. Bityurin^a,
V. V. Nemov^b, Yu. V. Sergeev^c, and M. A. Ostrovsky^d

^a Institute of Applied Physics, Russian Academy of Sciences, Nizhni Novgorod, 603950 Russia

^b Blokhina Institute of Epidemiology and Microbiology, Nizhni Novgorod, 603950 Russia

^c National Eye Institute, NIH, Bethesda, MD 20892-2510

^d Emmanuel Institute of Biochemical Physics, Russian Academy of Sciences, Moscow, 119334 Russia

Received November 6, 2007

Abstract—Here we compile and analyze the data on photoaggregation of a model protein carboanhydrase and the main eye lens proteins α -, β -, γ -crystallins under the action of pulsed UV irradiation from a Xe–Cl laser (308 nm) with broad variation of pulse energy density and repetition rate. The aggregation efficacy proves to be a nonlinear function of these parameters and protein concentration. A theoretical model is proposed that qualitatively explains the experimental data. It is shown that N-arm-truncated β A3-crystallin is more prone to UV-induced aggregation than the full-sized protein; such defects caused by mutation or aging may aggravate the development of lenticular opacity. Analyzed is the effect of some low-molecular compounds on the aggregation of β -crystallin and its mixture with α -crystallin. A combination of short peptides prepared on this basis markedly impedes crystallin aggregation and retards the development of UV-induced cataract in rats.

Key words: eye lens crystallins, photoaggregation, anti-cataract agents

DOI: 10.1134/S0006350908040064

INTRODUCTION

The eye lens in vertebrates is mostly composed of α -, β , and γ -crystallins; these proteins are about equally represented but differ in structure and size.

Various physical factors, e.g. UV radiation or elevated temperature, can cause aggregation of crystallins into large light-scattering conglomerates; this results in lenticular opacity, i.e., cataract [1–6]. Photoaggregation is characteristic of UVA/B, whereas UVC mostly causes photolysis, as demonstrated, e.g., in pig lens exposed to irradiation at 308 and 266 nm [7].

Cataract is the main cause of the loss of vision in humans. Now there are about 20 million persons afflicted worldwide, and the share of cataract in eye morbidity is 42% by the WHO data [8]. The treatment for this pathology is surgical: replacement of the opaque lens with an elastic implant. The techniques are well developed, but still have shortcomings (reviewed in [8]) such as secondary cataract, accommodation problems and astigmatism of the artificial lens. Therefore, very topical is the search for conservative and preventive anti-cataract treatment.

Lenticular opacity may be caused both by genetic and by external factors. One of the external factors of age-related cataract is the exposure of the lens to UV radiation of 290–320 nm [9, 10]. In this range of solar radiation incident on Earth ($2 \cdot 10^{-4}$ W/cm²) the human lens experiences a density of 10^{-7} to 10^{-6} W/cm² [11].

Taking 240 sunny days a year, we can estimate the annual exposure at about 10 J/cm². Here we present the data on the aggregation of crystallins exposed to monochromatic pulsed radiation at 308 nm with characteristic doses ~ 100 J/cm². The 308 nm light is weakly absorbed by these proteins, but at shorter wavelengths the absorption rises appreciably, which may speed up aggregation. Another difference from [11] is that the native lens has metabolic systems protecting it from external influences. However, our in vitro model experiments have produced data of interest both for the theory of protein photoaggregation and for practical medicine.

Light scattering can also arise because of perturbation of the lens cell order (impaired development or uncontrolled cell division) as well as loss of transparency by individual cells. Mutant crystallins may cause hereditary cataract because of altered stability, solubility, or intermolecular interaction. Photoaggregation was compared [12, 13] for recombinant β A3-crystallin and its mutant truncated in the amino arm (β A3tr). Such defects, observed in senile and cataract lenses, proved to accelerate photoaggregation.

The literature provides practically no information on the molecular mechanisms of UV-induced aggregation of crystallins, though this is important both in the basic and in the applied aspects. A step in this direction has been made in our works [14–17] with carboanhy-

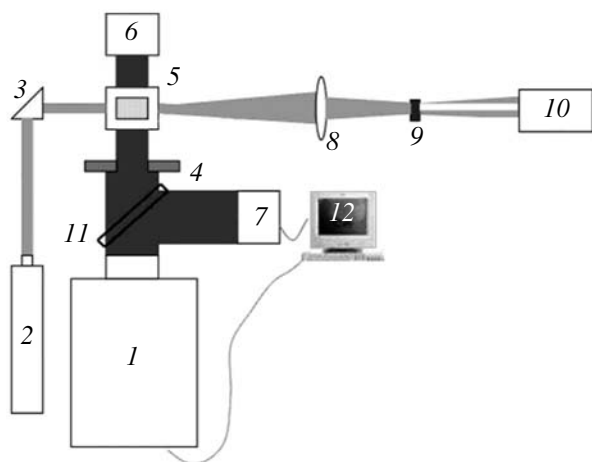


Fig. 1. Scheme of the experimental setup: (1) Xe-Cl laser 308 nm; (2) He-Ne laser 633 nm; (3) prism; (4) diaphragm; (5) test cuvette; (6, 7) UV energy meters; (8–10) lens, screen, and photodiode; (11) quartz plate (splitter); (12) automation system.

drase (CA), which nicely models β L-crystallin in the response of visible light scattering to the UV dose [4]. In the earlier studies that we are aware of, use was made of either continuous light from a mercury lamp [18–21] or laser pulses of fixed energy (w) and repetition rate (F) [2–5]. Varying these parameters in a broad range [14–17], we observed nonlinear behavior of the CA aggregation rate, and proposed a theoretical model assuming that aggregation occurs upon interaction of a pair of protein molecules each activated by an absorbed UV quantum and existing in the activated state for a finite time. This model, considering only dimerization, already provided a qualitative description of the experimental data. Previously, nonlinear dependences of the aggregation on w and F of laser pulses were reported for pig lens [7] and for bovine β -crystallin [6] as well as recombinant β A3 expressed and isolated as in [23].

γ -Crystallin is the most prone to aggregation, followed by β -crystallin [2, 3, 6], whereas α -crystallin has chaperone activity and impedes aggregation of these proteins under the action of UV light and other denaturing factors (heating, S-S reducers) [4, 24]. The chaperone activity of α -crystallin is believed to decline with age, which may contribute to senile cataract [25]. Hence, the search for new anti-cataract agents should concern substances that directly retard aggregation of β - and γ -crystallins and those that sustain the protective function of α -crystallin. It has been shown in vitro [26] that D-pantethine (dimeric vitamin B5-cysteamine conjugate) and related compounds slow down the thermal aggregation of a β/α -crystallin mixture. Anti-cataract properties have also been assessed for L-carnosine (β Ala-His) and N-acetyl carnosine [27].

Here we summarize and analyze our results on UV-induced aggregation of CA and different crystallins as well as the protective effects of a novel formulation of

short peptides [28–30] in comparison with patented anti-cataract drugs [31, 32].

EXPERIMENTAL

Carboanhydrase, crystallins, and low-molecular compounds were from Sigma-Aldrich (St. Louis, MO) and Hamari Chemicals (Japan). Proteins were dissolved to 0.5 mg/ml in phosphate buffer, pH 7.2 with 150 mM NaCl, passed through 0.45- and 0.22- μ m membrane filters (Sartorius, Germany), and centrifuged for 15 min at 5000 g, discarding the bottom part of the supernatant. Recombinant β A3 and β A3tr were expressed and isolated as described [23, 34–36] and diluted in PBS with 1 mM DTT and 50 μ M tris(2-carboxyethyl)phosphine (TCEP; Pierce, Rockford, IL). All analytical procedures have also been described elsewhere [6, 13–17].

The scheme of the setup is shown in Fig. 1. The 308 nm UV source was (1) an excimer Xe-Cl laser LPX-200 (Lambda Physik, Germany). Experiments were done at $(22 \pm 1)^\circ\text{C}$; the heating of protein samples under irradiation did not exceed 2°C . The UV dose was determined as $D = wFt$ (t is exposure time). Pulse energy was determined with a patented [37] meter (7). A He-Ne laser (2) (10 mW, 633 nm, beam divergence of 1.1 mrad) was used as a test beam to assay light scattering in a direction perpendicular to the UV laser beam (photodiode 10); simultaneously, the energy of UV pulses transmitted through the cuvette (5) was measured with a Gentec (Canada) ED-200 device (6). The optical paths of the cuvette (5) along the Xe-Cl and He-Ne laser beams were 10 and 5 mm, respectively. Data from the pickups (6, 7, 10) were continuously processed by an automation system (12) with averaging over a preset pulse number. The results were displayed in graphic form.

RESULTS AND DISCUSSION

Aggregation of Carboanhydrase and Crystallins

Exposure of protein solutions to intense laser radiation can cause processes that do not take place in the lens exposed to natural sunlight. First of all, this concerns nonlinear, e.g. two-photon absorption. In our experiments, the UV absorption coefficient was about $5 \cdot 10^{-2} \text{ cm}^{-1}$ and remained constant at w ranging from 2 to 300 mJ/cm^2 , thus excluding nonlinear two-photon absorption.

Scattering of visible light upon variation of UV parameters was examined with the CA model. The data for the power P scattered by 0.5 mg/ml CA at different w and F are given in Fig. 2. One of the main characteristics of aggregation is the threshold dose D^* at which the $P(D)$ dependence starts to rise. For every w there is a threshold F^* below which D^* is great. Thus at $w = 40 \text{ mJ}/\text{cm}^2$ (Fig. 1a) we see the same D^* of $\sim 250 \text{ J}/\text{cm}^2$ for $F = 6\text{--}16 \text{ Hz}$, but for $F = 4 \text{ Hz}$ the D^* rises to ~ 400 and exceeds $800 \text{ mJ}/\text{cm}^2$ for $F = 3 \text{ Hz}$. To add, at low F

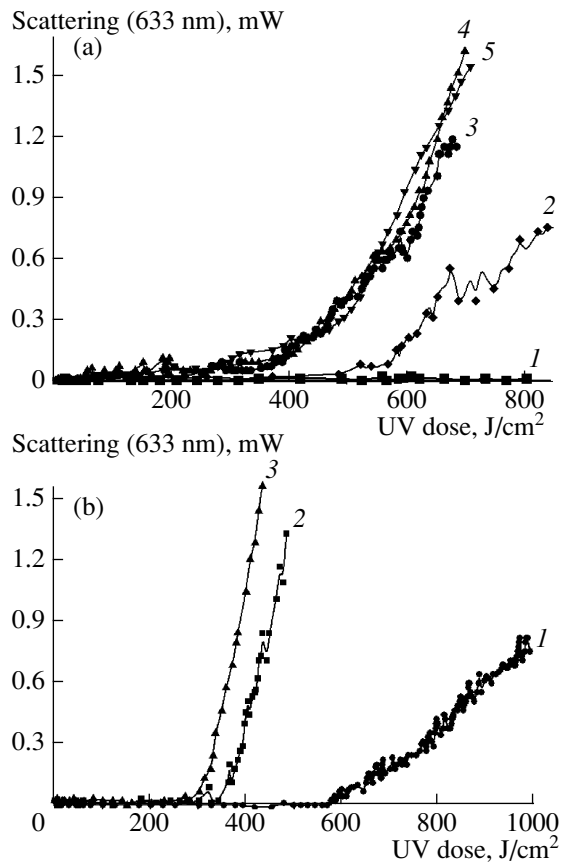


Fig. 2. Dependences of the power of 633 nm light scattered in carboanhydrase solution on the UV irradiation dose at different pulse energy density w and repetition rate F . (a) $w = 40 \text{ mJ/cm}^2$, (1) 3, (2) 4, (3) 6, (4) 10, (5) 16 Hz; (b) $w = 84 \text{ mJ/cm}^2$, (1) 1, (2) 2, (3) 4 Hz.

the $P(D)$ slope is also small. This means that the protein aggregation efficacy is low at $F < F^*$. On the other hand, at $F > F^*$ neither the D^* nor the slope depend on F . In Figs. 3–5, the $D^*(w)$, $D^*(F)$, $F^*(w)$ and mean intensity $p^*(w)$ [$p^* = F^* w$] plots demonstrate the non-linear dependence of CA aggregation on the UV pulsing regime. Note that a similar $D^*(w)$ behavior was observed earlier [7] for pig lens irradiated at 308 nm, whereas at 266 nm, with prevalent photolysis, $D^*(w)$ was constant.

Protein aggregation must alter the size of dissolved particles. This was confirmed by gel filtration of CA before and after exposure to $0.1D^*$ (Fig. 6). One can see that a dimer peak (58 kDa) develops and larger forms appear at a dose that does not yet cause light scattering.

A comparative study of UV-induced aggregation of crystallins [6] revealed that its rate [per unit energy] was lowest for α -, higher for β L-, and still higher for γ -crystallin (Fig. 7), in line with earlier data [2]. The same work [6] showed very similar dynamics for bovine lens β L-crystallin and the recombinant β A3 protein.

Figure 8 shows that the β A3 aggregation rate strongly depends on protein concentration. At 1.0 or

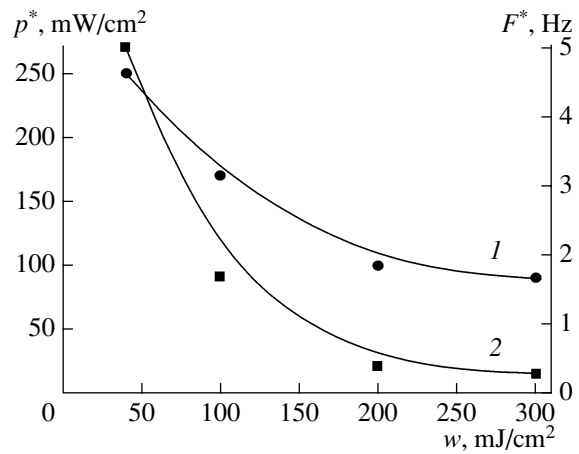


Fig. 3. Dependence of (1) threshold intensity p^* and (2) pulsing rate F^* on pulse energy density w ($p^* = F^* w$).

0.8 mg/ml aggregation is virtually steady with $D^* \sim 50 \text{ J/cm}^2$, but at 0.2 mg/ml $D^* > 1000 \text{ J/cm}^2$; i.e., a 1:4 dilution impedes the aggregation more than 20 times (the $D^*(C_0)$ plot is Fig. 9).

Figure 10 shows the dose–response curves for β L and β A3 in two irradiation regimes: (a) at $C_0 = 0.5 \text{ mg/ml}$, $w = 75 \text{ mJ/cm}^2$, $F = 2 \text{ Hz}$, we see that $D^* \sim 60 \text{ J/cm}^2$; whereas (b) at 0.8 mg/ml, $w = 2.5 \text{ mJ/cm}^2$, $F = 50 \text{ Hz}$, the $D^* \sim 250 \text{ J/cm}^2$. This means that the irradiation efficacy is much higher with more intense but rarer pulses.

Figure 11 presents the elution profiles for β A3 irradiated to different UV doses in the $w = 75 \text{ mJ/cm}^2$, $F = 2 \text{ Hz}$ regime. Just as with CA, there is a progressive decline in the initial peak and accumulation of a twice-larger species at doses below the light scattering threshold.

Analysis of UV-irradiated β A3 by gel filtration and SDS-PAGE suggested (i) dimerization and further aggregation at low doses, and (ii) prevalent photolytic rupture of the polypeptide at high doses [6].

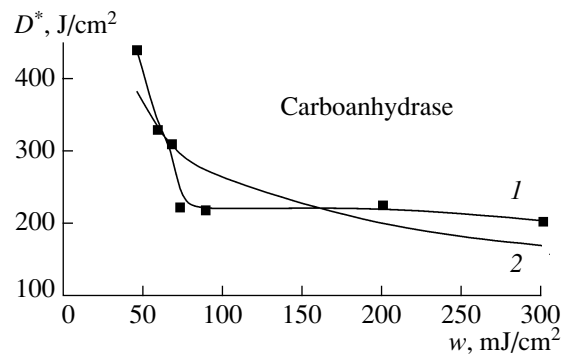


Fig. 4. Dependence of threshold dose D^* on w at $F = 2 \text{ Hz}$: (1) experiment, (2) theoretical curve.

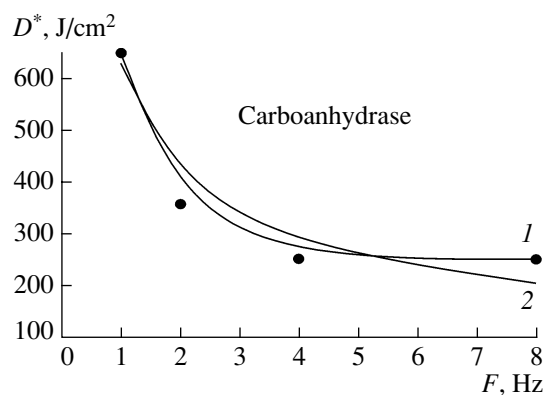


Fig. 5. Dependence of threshold dose D^* on F at $w = 70 \text{ mJ/cm}^2$: (1) experiment, (2) theoretical curve.

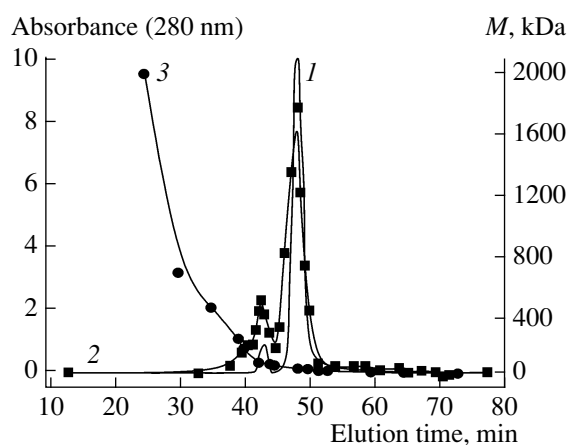


Fig. 6. Gel filtration (Superose 12 10/30 HR, 0.3 ml/min) of carboanhydrase (1) before and (2) after UV irradiation to $D = 0.1D^*$; (3) size markers.

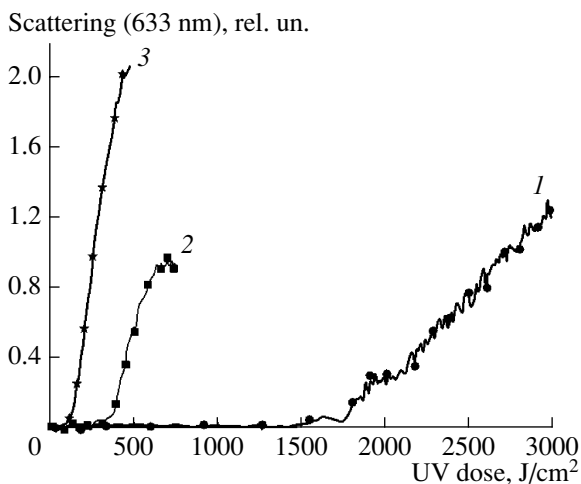


Fig. 7. Different sensitivity of (1) α -, (2) β -, and (3) γ -crystallins to UV irradiation ($w = 2.5 \text{ mJ/cm}^2$, $F = 50 \text{ Hz}$). Taken from [6] with Journal's permission.

Detailed analysis of light scattering by βL -crystallin irradiated in various regimes [22] revealed $P(D)$ patterns qualitatively identical to those described above for CA, with interdependent F and w thresholds (Figs. 12–15). Thus, UV-induced aggregation of βL -crystallin can also be roughly described with the simplified model assuming interaction of two activated molecules (see last section). This model also accommodates the concentration dependence for βA3 (Fig. 9): indeed, a decrease of C_0 , just as a decrease of w or F , would lower the probability of protein association.

The transmission spectra of native and increasingly irradiated βL solutions (Fig. 16) proved similar to those of CA, and the difference spectrum of induced absorption (dashed) was analogous to the one obtained earlier [18] for the water-soluble fraction of bovine lens, with a characteristic peak at 305 nm.

Gel filtration showed that increasing exposure to UV light leads to a decline in the initial βL peak of 45 kDa, with simultaneous broadening toward larger size; at $0.5D^*$ the protein appears in the void volume ($\geq 2000 \text{ kDa}$) and accumulates there at higher doses. Thus, aggregation of βL as well as of βA3 and CA commences at UV exposures that do not yet produce detectable light scattering.

Besides external factors, cataract can be caused by internal alterations such as mutations. Thus some βA3 mutations have been associated with autosomal dominant zonular cataract [38–41]; numerous other works (cited in [13]) associate structural changes of various crystallins with hereditary cataracts. Supposing that such structural alterations make crystallins more susceptible to UV damage [13], we compared the responses of βA3 and βA3tr (modeling the N-arm loss observed in lens aging and cataract). As evident from Figs. 17 and 18, the impaired protein was indeed considerably more prone to photoaggregation.

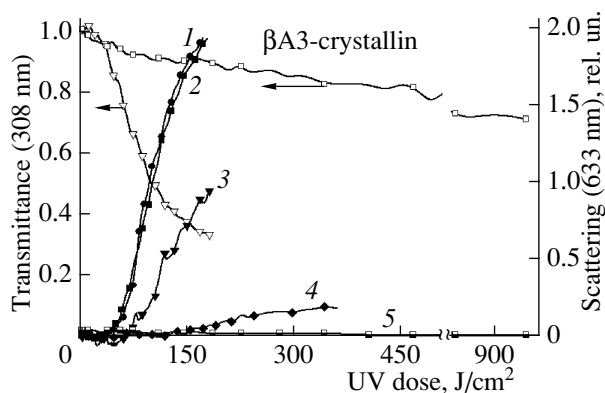


Fig. 8. Dose dependences of visible light scattering and UV transmission in βA3 -crystallin solutions of (1) 1, (2) 0.8, (3) 0.6, (4) 0.4, and (5) 0.2 mg/ml; $w = 75 \text{ mJ/cm}^2$, $F = 2 \text{ Hz}$.

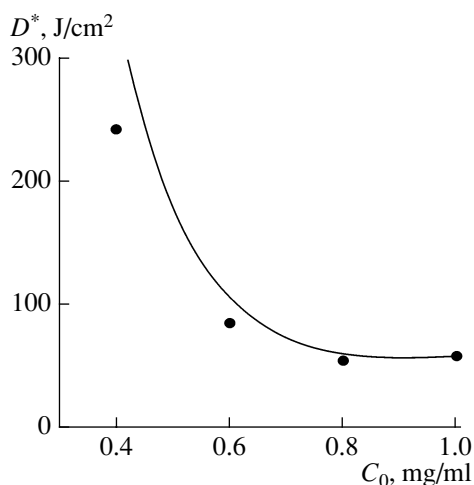


Fig. 9. Concentration dependence of D^* (data of Fig. 8).

Effect of Low-Molecular Compounds on Crystallin Aggregation

Further, we examined the influence of a number of low-molecular compounds on the aggregation of β L-crystallin and its mixtures. Figure 19 shows the significant effect of D-pantethine on the $P(D)$ in an $\alpha\beta\gamma$ mixture that is close to the composition of the lens proteins.

Detailed comparative analysis was performed for the mixture of β L- with α -crystallin; Fig. 20 confirms that α -crystallin is less prone to aggregation and has a protective effect on β L (owing to its chaperone-like activity). We have determined the compounds that directly retard the aggregation of β L-crystallin or reinforce the α -crystallin activity, and designed a combination of such substances [28–30] (further referred to as the novel formulation, NF) that in vitro proved superior to the basic components of patented anti-cataract drugs [31, 32] pantethine or (N-acetyl)arnosine. Below we show the data only for these three most effective agents (arnosine itself had about the same effect). We have recently demonstrated [42] that the protective action of N-acetylarnosine is due not to antioxidant but to antiaggregative properties analogous to those of α -crystallin.

Figure 21 shows that NF increases the threshold UV dose for light scattering much more than either pantethine or N-acetylarnosine. Likewise, it clearly suppresses the appearance of high-molecular aggregates in the β/α mixture (Fig. 22).

Figure 23 summarizes the chromatographic data processed to represent the decline in the monomeric β L and the accumulation of large aggregates at increasing UV irradiation without and with protective agents. In full accord with Fig. 21, NF is the most efficient in retarding crystallin aggregation.

In parallel with the scattering of visible light, we monitored the transmission of UV pulses. Attenuation in crystallin solutions at low doses (relative transmittance down to 0.8–0.7) is probably due to photochemi-

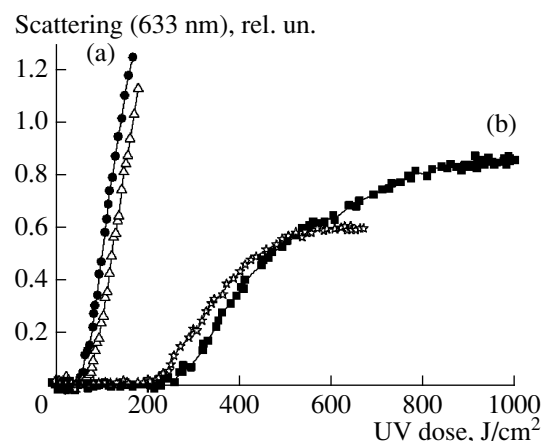


Fig. 10. Dose dependences of β L and β A3-crystallin aggregation at (a) $C_0 = 0.5$ mg/ml, $w = 75$ mJ/cm², $F = 2$ Hz; (b) $C_0 = 0.8$ mg/ml, $w = 2.5$ mJ/cm², $F = 50$ Hz. Adapted from [6].

cal reactions, and the dose–transmittance curves are well approximated with an exponential function (Figs. 12b, 14, 20). For β L-crystallin these changes correspond to the transmission spectra in Fig. 16. If no aggregation is caused by UV irradiation (low w , F , or low C_0 as exemplified in Fig. 8), the transmittance curve is monotonous. The onset of aggregation is attended by more pronounced UV attenuation mostly due to scattering, and this is seen as an inflection in the transmittance curve. Figure 24 shows that pantethine or NF added to the β L/ α mixture shift the inflection point to higher UV doses, which fully agrees with the $P(D)$ curves and the chromatographic data.

The NF has been tested in the Institute of Eye Diseases, Moscow on male Wistar rats using different administration regimens, and in all cases produced a positive effect (retardation of UV-induced cataract)

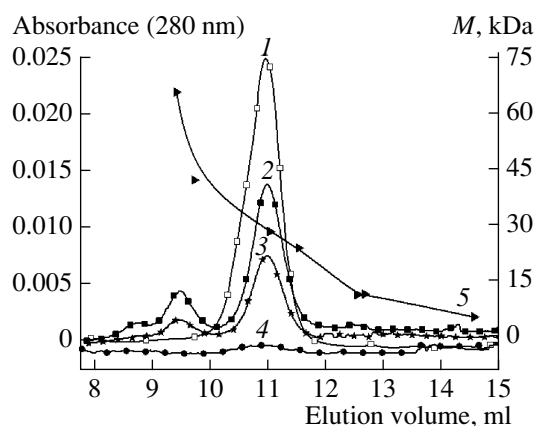


Fig. 11. Gel filtration (Superdex 75 10/30 HR, 0.5 ml/min) of β A3-crystallin before (1) and after UV irradiation to a D of (2) 26, (3) 50, and (4) 170 J/cm²; (5) size markers. Taken from [6] with Journal's permission.

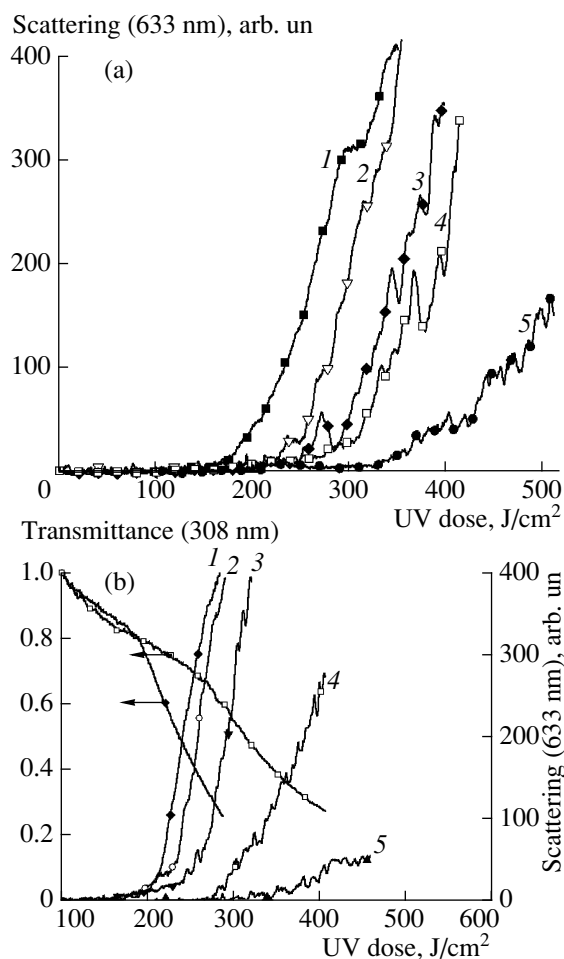


Fig. 12. Dependences of the power of 633 nm light scattered in β L-crystallin solution on the UV irradiation dose at different pulse energy density w and repetition rate F . (a) $w = 40$ mJ/cm², (1) 9, (2) 6, (3) 4, (4) 3, (5) 2 Hz; (b) $w = 75$ mJ/cm², (1) 4, (2) 2, (3) 1.5, (4) 1, (5) 0.7 Hz; transmission at 308 nm is also shown.

[33]. Thus, it holds promise as regards prevention of cataract in humans.

PHOTOAGGREGATION MODEL

The experimental data and their relevance to crystallin aggregation under natural sunlight can be explained assuming that aggregation can occur by interaction between two photoactivated molecules but also between an activated and an intact molecule. The former process perhaps prevails upon laser irradiation, which causes massive activation, whereas the latter may be prevalent under normal illumination. Taking R and M to represent the concentrations of the activated and the aggregated proteins, the kinetic description is

$$\frac{dR}{dt} = \eta\sigma C_0 \frac{I}{\hbar\omega} - k_2 R^2 - k_1 C_0 R - \frac{R}{\tau},$$

$$\frac{dM}{dt} = k_2 R^2 + 2k_1 C_0 R. \quad (1)$$

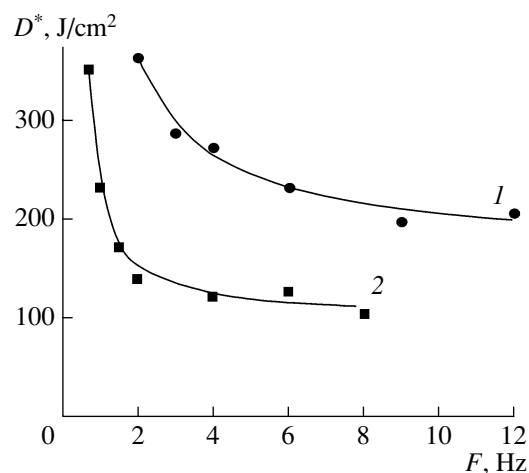


Fig. 13. Experimental (points) and theoretical (lines) dependence of threshold dose D^* on F for 0.5 mg/ml β L-crystallin at $w = (1)$ 40 and (2) 75 mJ/cm².

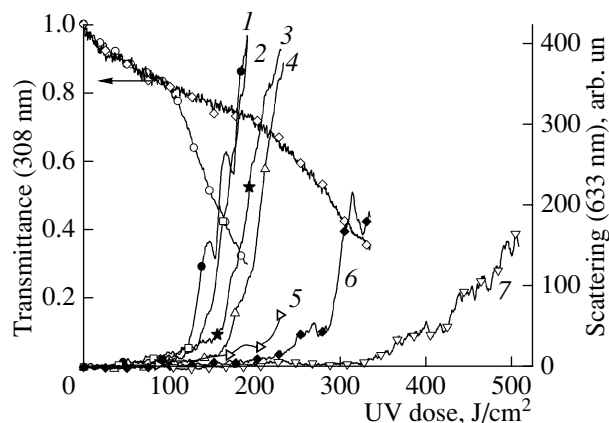


Fig. 14. Dose dependences of visible light scattering and UV transmission in β L-crystallin solutions (0.5 mg/ml) at $F = 2$ Hz and w of (1) 90, (2) 80, (3) 75, (4) 70, (5) 60, (6) 50, and (7) 40 mJ/cm².

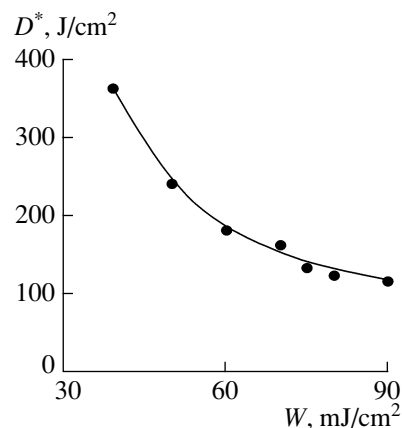


Fig. 15. Experimental (points) and theoretical (line) dependence of threshold dose D^* on w at $F = 2$ Hz for 0.5 mg/ml β L-crystallin.

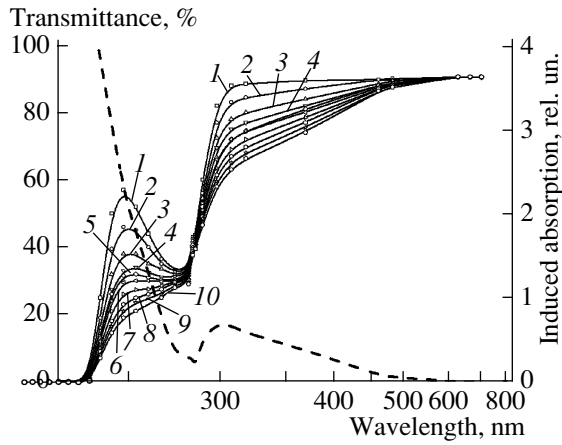


Fig. 16. Optical transmission spectra of β L-crystallin solutions (0.5 mg/ml, 1 cm light path) before (1) and after UV irradiation to a D of (2) 1/6, (3) 1/3, (4) 1/2, (5) 2/3, (6) 5/6, (7) 1, (8) 7/6, (9) 4/3, and (10) $3/2 D^*$; the dashed line is the induced absorption (difference between 10 and 1).

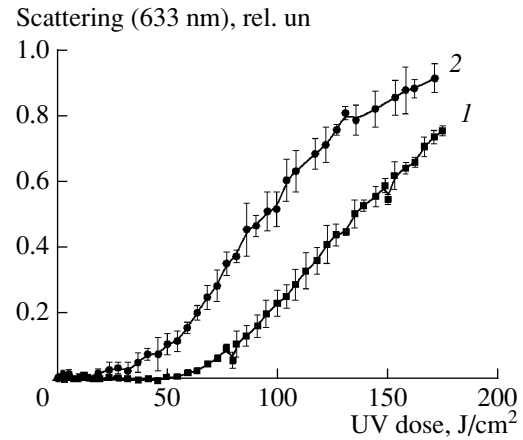


Fig. 17. Dose dependences of visible light scattering by (1) normal β A3-crystallin and (2) mutant β A3tr. Taken from [13] with Journal's permission.

Here C_0 is the monomer concentration (neglecting its change during aggregation), I is UV intensity (which, generally speaking, is time-dependent), $\hbar\omega$ is the light quantum energy, σ is the effective section of UV absorption by monomers, η is the quantum yield of photoactivation, k_2 is the dimerization rate constant for two activated monomers, k_1 is the constant for dimerization between an activated and an intact monomer. For simplicity, we disregard at the initial stage the attachment of activated molecules to the aggregates. An important parameter of the model is the characteristic lifetime of the activated state (τ).

To understand the basic properties of the model, let us consider continuous irradiation ($I = \text{const}$). From the analysis of protein photoaggregation kinetics it follows that

$$k_1 C_0 \ll \tau^{-1}. \quad (2)$$

We have established that under intense laser irradiation

$$k_1 C_0 R \ll k_2 R^2. \quad (3)$$

The concentration of activated monomers quickly reaches a steady state $R = R_C$ found from the first equation (1) by zeroing the time derivative. Neglecting the term $k_1 C_0 R$ in (1), for the laser case we get

$$R_C = (2k_2\tau)^{-1} (\sqrt{1 + III_0} - 1). \quad (4)$$

which includes the characteristic intensity

$$I_0 = \frac{\hbar\omega}{\eta\sigma C_0 4k_2\tau^2}. \quad (5)$$

Taking that the onset of visible light scattering corresponds to accumulation of a certain concentration of

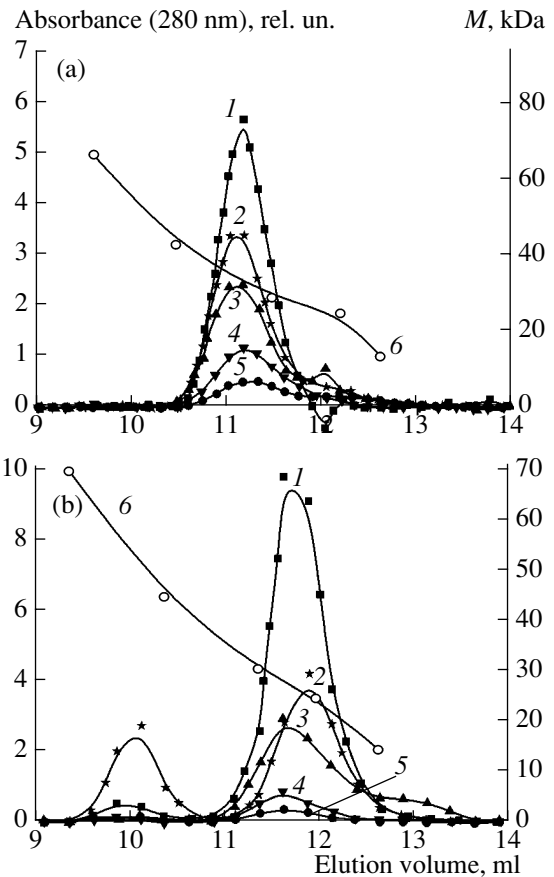


Fig. 18. Gel filtration (Superdex 75 10/30 HR, 0.5 ml/min) of (a) BA3 and (b) β A3tr crystallins before (1) and after UV irradiation to a D of (2) 25, (3) 50, (4) 125, and (5) 200 J/cm^2 ; (6) size markers. Taken from [13] with Journal's permission.

aggregates M^* , the threshold UV dose can be estimated

$$\text{from the second equation (1) as } D^* \approx \frac{M^* I}{k_2 R_C^2} \text{ or}$$

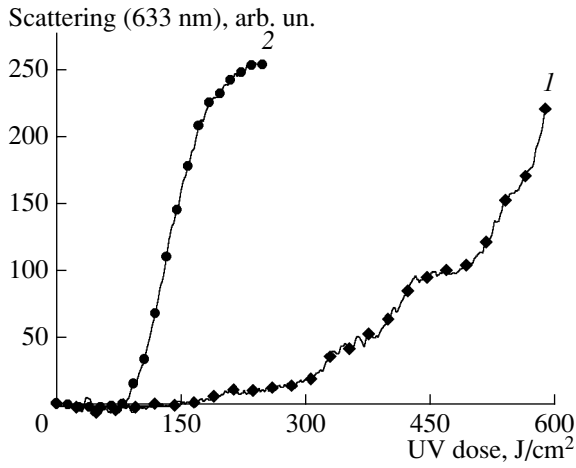


Fig. 19. Influence of D-pantethine (1) on UV-induced aggregation in a mixture of α -, β L-, and γ -crystallins (2). Each component at 0.5 mg/ml.

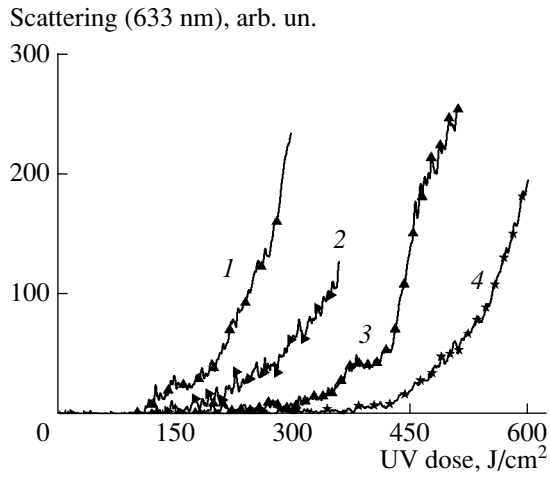


Fig. 21. UV-induced aggregation in a mixture of β L- and α -crystallins without (1) and with (2) D-pantethine, (3) N-acetyl carnosine, and (4) novel formulation. Each component at 0.5 mg/ml.

$$D^* \approx \frac{4k_2\tau^2 M^* I}{(\sqrt{1 + I/I_0} - 1)^2}. \quad (6)$$

From (6) it follows that at relatively high intensity ($I \gg I_0$) we have $\sqrt{1 + I/I_0} - 1 \approx \sqrt{I/I_0}$ and

$$D^* \approx 4k_2\tau^2 M^* I_0 = \frac{\hbar\omega M^*}{\eta\sigma C_0}. \quad (7)$$

i.e., D^* does not depend on UV intensity.

In the other limit case, if $I \ll I_0$ but condition (3) holds (as shown below, this means $I \gg 4\tau k_1 C_0 I_0$) we get

$$\sqrt{1 + I/I_0} - 1 \approx \frac{I}{2I_0} \text{ and}$$

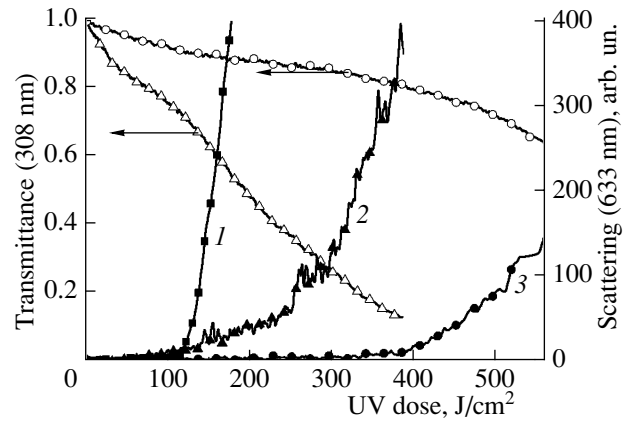


Fig. 20. Dose dependences of visible light scattering and UV transmission in solutions of crystallins (1) β , (2) $\beta + \alpha$, (3) α .

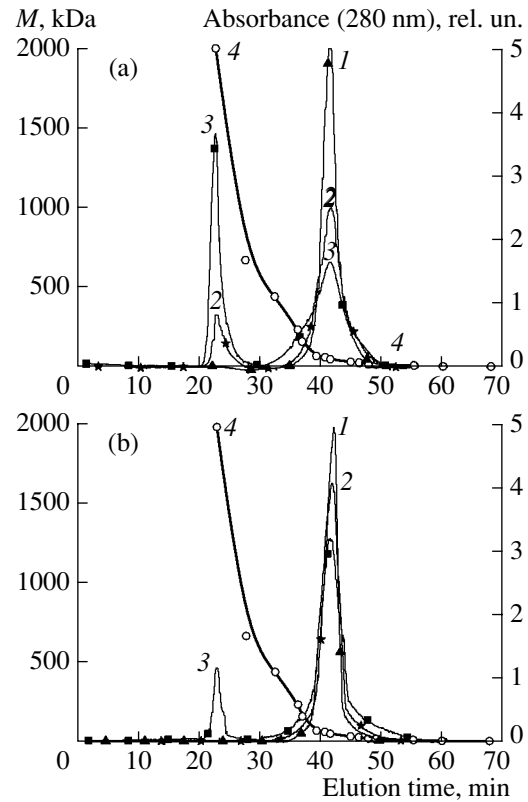


Fig. 22. Gel filtration (Superose 12 10/30 HR, 0.3 ml/min) of α/β L-crystallin mixture (a) alone or (b) with NF: before (1) and after UV irradiation to (2) 50 and (3) 85 J/cm²; (4) size markers. Data only for intact β L (45 kDa) and large aggregates (≥ 2000 kDa).

$$D^* \approx \frac{1}{I} 16k_2\tau^2 M^* I_0^2 = \frac{M^*}{Ik_2\tau^2} \left(\frac{\hbar\omega}{\eta\sigma C_0} \right)^2. \quad (8)$$

Thus, at low enough intensities D^* is inversely proportional to I . The kinetic features following from (7) and (8) are observed experimentally (Figs. 4, 5 for CA

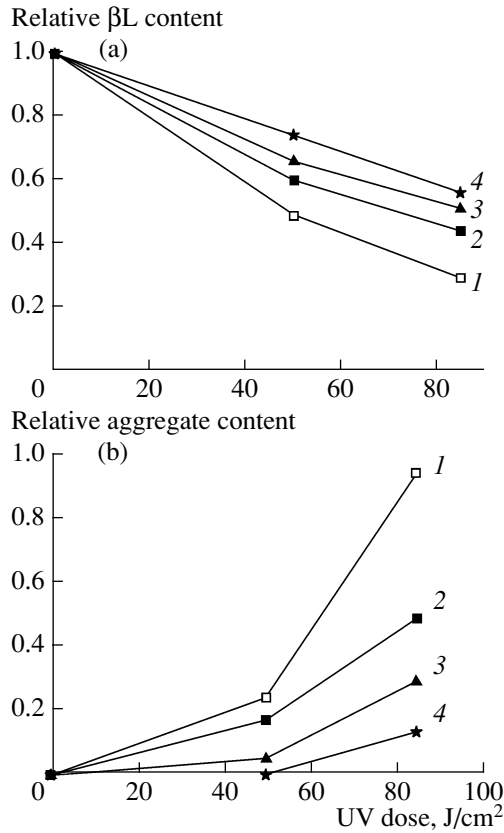


Fig. 23. Dose dependences for the contents of (a) intact and (b) highly aggregated β L-crystallin (chromatographic data) upon UV irradiation of the α/β L mixture (1) alone or with (2) D-pantethine, (3) N-acetyl carnosine, and (4) NF.

and Figs. 13, 15 for β L-crystallin), confirming the validity of the main model premises.

From (8) it also follows that an increase in the relaxation time τ must decrease D^* . In this respect, the protective activity of our additives may be interpreted as their influence on τ .

Now consider the low-intensity case corresponding to natural light. R must be low, so in set (1) we can ignore all quadratic terms, i.e.,

$$k_1 C_0 R \gg k_2 R^2. \quad (9)$$

With (2) for the steady state we get

$$R_C = \eta \sigma C_0 \frac{I}{\hbar \omega} \tau. \quad (10)$$

We can rewrite (9) as

$$I \ll \frac{k_1 \hbar \omega}{\tau k_2 \eta \sigma} = 4 \tau k_1 C_0 I_0. \quad (11)$$

From the second equation (1) we obtain

$$D^* \approx \frac{\hbar \omega}{2 \eta \sigma k_1 C_0} \frac{M^*}{1}. \quad (12)$$

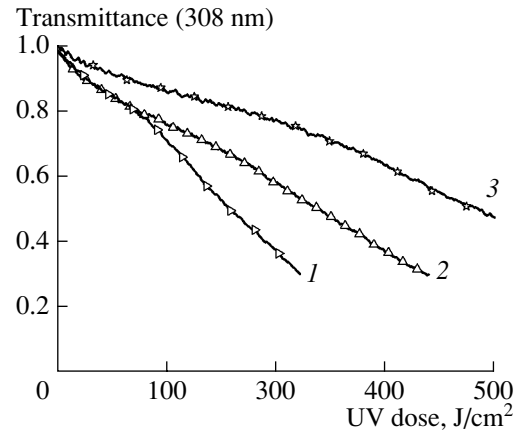


Fig. 24. Dose dependence of UV transmission through the α/β L mixture (1) alone, (2) with D-pantethine, or (3) with NF.

i.e., $D^* \sim \tau^{-1}$. Shortening the relaxation time, we raise the threshold and suppress protein aggregation. This means that the most effective additives selected in laser experiments must be also effective against natural low-intensity irradiation.

ACKNOWLEDGMENTS

The authors are grateful to K.O. Muranov for advice and discussion.

The work was supported by the RAS programs Basic Science for Medicine, Biomolecular and Medical Chemistry, and RFBR (05-04-48749a, 05-04-49945a, 06-02-17381a, 06-04-08232).

REFERENCES

1. A. V. Krivandin, Yu. M. Lvov, M. A. Ostrovski, et al., *Exp. Eye Res.* **49**, 853 (1989).
2. J. L. Hott and R. F. Borkman, *Photochem. Photobiol.* **57**, 312 (1993).
3. D. Y. Li, R. F. Borkman, R. H. Wang, and J. Dillon, *Exp. Eye Res.* **51**, 663 (1990).
4. R. F. Borkman, G. Knight, and B. Obi, *Exp. Eye Res.* **62**, 141 (1996).
5. U. P. Andley, M. A. Sawardekar, and J. L. Burris, *Photochem. Photobiol.* **65**, 556 (1997).
6. M. A. Ostrovsky, Y. V. Sergeev, D. L. Atkinson, et al., *Molecular Vision* **8**, 72 (2002).
7. N. M. Bityurin, S. V. Muraviov, V. A. Kamensky, et al., *Proc. SPIE* **4161**, 1 (2000).
8. B. E. Malyugin, *Vestn. Oftal'mol.* no. 1, 37 (2006).
9. J. Blondin, V. Baragi, E. Schwartz, et al., *J. Free Rad. Biol. Med.* **2**, 275 (1986).
10. A. Taylor, *Nutr. Rev.* **47**, 225 (1989).
11. S. Zigman, *Optom. Vis. Sci.* **72**, 899 (1995).
12. Y. V. Sergeev, L. V. Soustov, E. V. Chelnokov, et al., *Abstracts of ARVO* (Florida, USA, 2003).
13. Yu. V. Sergeev, L. V. Soustov, E. V. Chelnokov, et al., *Investigat. Ophthalmol. Visual Sci.* **46**, 3263 (2005).

14. N. M. Bityurin, L. V. Soustov, and E. V. Chelnokov, Preprint 599 (Inst. Appl. Phys., Nizhni Novgorod, 2002).
15. L. V. Soustov, E. V. Chelnokov, N. M. Bityurin, et al., Dokl. RAN **388**, 683 (2003).
16. L. V. Soustov, E. V. Chelnokov, N. M. Bityurin, et al., Technical program of IQEC/LAT (International Quantum Electronics Conference) (2002).
17. L. V. Soustov, E. V. Chelnokov, N. M. Bityurin, et al., Proc. SPIE **5149**, 85 (2003).
18. M. M. Korkhmazyan, I. B. Fedorovich, and M. A. Ostrovskii, Biofizika **28**, 966 (1983).
19. V. V. El'chaninov and K. B. Fedorovich, Biofizika **34**, 758 (1989).
20. V. V. El'chaninov and K. B. Fedorovich, Biofizika **35**, 200 (1990).
21. M. A. Ostrovskii, K. B. Fedorovich, V. V. El'chaninov, et al., Sensornye Sistemy **8(3-4)**, 135 (1994).
22. L. V. Soustov, E. V. Chelnokov, N. M. Bityurin, et al., Proc. SPIE **5506**, 28 (2004).
23. J. N. Hope, H. C. Chen, and J. F. Hejtmancik, Protein Eng. **7**, 445 (1994).
24. J. Horwitz, Proc. Natl. Acad. Sci. USA **89**, 10449 (1992).
25. M. Cherian and E. G. Abraham, Biochem. Biophys. Res. Comm. **208**, 675 (1995).
26. J. I. Clark and Q. L. Huang, Proc. Natl. Acad. Sci. USA **93**, 15185 (1996).
27. A. A. Boldyrev, *Carnosine: Biological Significance and Medical Applications* (Izd. MGU, Moscow, 1998) [in Russian].
28. L. V. Soustov, E. V. Chelnokov, K. M. Bityurin, et al., *Abstracts of Conference "Basic Science for Medicine"* (Slovo, Moscow, 2004), pp. 192–194 [in Russian].
29. L. V. Soustov, E. V. Chelnokov, K. M. Bityurin, et al., Technical program of IQEC/LAT. (International Quantum Electronics Conference) (2005).
30. L. V. Soustov, E. V. Chelnokov, A. L. Kiselev, et al., Proc. SPIE **6257**, 62570X1 (2006).
31. J. I. Clark, G. B. Benedek, R. J. Siezen, et al., US Patent 5.091.421 (1992).
32. A. A. Boldyrev, A. A. Ragimov, and V. E. Formazyuk, RF Patent 2071316 (1993).
33. S. E. Avetisov, G. S. Polunin, N. L. Sheremet, et al., Vestn. Oftal'mol. **124** (2), 12 (2008).
34. Y. V. Sergeev, P. T. Wingfield, and J. F. Hejtmancik, Biochemistry **39**, 15799 (2000).
35. Y. V. Sergeev, J. F. Hejtmancik, and P. T. Wingfield, Biochemistry **43**, 415 (2004).
36. J. N. Hope, H.-C. Chen, and J. F. Hejtmancik, J. Biol. Chem. **269**, 21141 (1994).
37. M. Yu. Kazakov, S. V. Murav'ev, and L. V. Soustov, RF Patent 2031378 (1991).
38. C. Kannabiran, P. K. Rogan, L. Olmos, et al., Mol. Vision. **4**, 21 (1998).
39. K. P. Burdon, M. G. Wirth, D. A. Mackey, et al., J. Ophthalmol. **88**, 79 (2004).
40. Y. Qi, H. Jia, S. Huang, et al., Hum. Genet. **114**, 192 (2004).
41. J. B. Bateman, D. D. Geyer, P. Flodman, et al., Invest. Ophthalmol. Vis. Sci. **41**, 3278 (2000).
42. K. O. Muranov, A. K. Timofeeva, A. A. Boldyrev, et al., Vestn. Oftal'mol. **124** (2), 3 (2008).